



## Bubbly flow characteristics during decompression sickness: Effect of surfactant and electrolyte on bubble size distribution

Sotiris P. Evgenidis, Nikolaos A. Kazakis, Thodoris D. Karapantsios\*

Department of Chemistry, Aristotle University of Thessaloniki, University Box 116, 541 24 Thessaloniki, Greece

### ARTICLE INFO

#### Article history:

Received 23 November 2009

Received in revised form 18 February 2010

Accepted 24 February 2010

Available online 3 March 2010

#### Keywords:

Bubbly flow

Bubble size

Surfactant

Electrolyte

Salinity

Decompression sickness

### ABSTRACT

This work presents experiments in a bubbly flow comparable to the one observed during decompression sickness (DCS) in humans. Experiments are conducted in a tube dimensionally similar to vena cava of the human body with liquids of various properties (surface tension, viscosity, conductivity) and liquid flow rates equivalent to those of human blood circulation. New data concerning the effect of separate and simultaneous presence of surfactant and electrolyte in the liquid phase on the bubble size distribution are acquired. In this respect, the influence of gas and liquid flow rates has also been studied. The results indicate a clear effect of surfactant concentration on bubble coalescence hindrance. Moreover, a synergy of surfactant and electrolyte is observed which is over and above their influence if they were alone in the liquid phase.

© 2010 Elsevier B.V. All rights reserved.

### 1. Introduction

Two-phase flow examples exist abundantly in technology and in nature as well (e.g. reactors, pipelines, rain). One of the simplest and most commonly observed types of two-phase flow is bubbly flow, which can be found in chemical, petrochemical and biological industry [1].

An interesting non-industrial example of bubbly flow is observed when decompression sickness (DCS) takes place. DCS is a clinical syndrome caused by rapid reduction of environmental pressure in the body that results in formation of bubbles within body tissues, creating symptoms of variable severity that range from joint pain to permanent deficits or even death. Bubbles are formed mainly in the skin, joints and the spinal cord and may move directly into the veins and altogether gather in vena cava before passing to the pulmonary filter [2]. Such situations may come up in the bloodstream of astronauts during extravehicular activity (EVA), because in that case crewmembers go from a cabin pressure of 14.7 psia, inside the space shuttle or international space station, to the space suit pressure of 4.3 psia [3]. All the above, together with the increasing need for EVAs in the following years, underline the importance of developing an in-vivo non-intrusive technique for the detection of bubbles in the body of astronauts in their space suits.

According to the aforementioned, it would be a great challenge to develop a technique able to detect bubbles inside the blood circulation system of the astronauts during EVAs. More specifically, an electrical technique, based on the different conductivity of the two phases, seems to be more appropriate, and it is indeed under development in our lab [4], since other existing methods display serious drawbacks. For example, the Doppler ultrasound method cannot track bubbles of size as small as those observed in DCS, while its sensitivity varies with bubble size [5]. However, to accomplish this and to test the validity of such an electrical technique, preliminary experiments must also be conducted in-vitro where the conditions (e.g. bubble size, gas volume fraction, blood properties and flow rates) of the bubbly flow inside the human body that prevail during the DCS are properly simulated.

It is widely accepted, that one of the most important parameters in a bubbly flow, namely the bubble size, is contingent to a great extent on the physical properties and the flow rates of the two phases. Specifically, the effect of additives in the liquid phase on the characteristics of the bubbly flow (e.g. bubble size, bubble coalescence) is a subject that has drawn the attention of researchers the last decades [6]. It seems that even small amounts of surfactant additives can drastically reduce bubble size and hinder coalescence between bubbles. Both effects are chiefly ascribed to surface tension decrease of the system (e.g. [7,8]). Alike are the results when inorganic salts are added in the liquid phase due to the electrostatic interaction between charged bubbles. Yet, their effects are noticeable only above a critical concentration (e.g. [9]). However, to the authors' best knowledge few are the studies which consider

\* Corresponding author. Tel.: +30 2310997772; fax: +30 2310997772.  
E-mail address: [karapant@chem.auth.gr](mailto:karapant@chem.auth.gr) (T.D. Karapantsios).

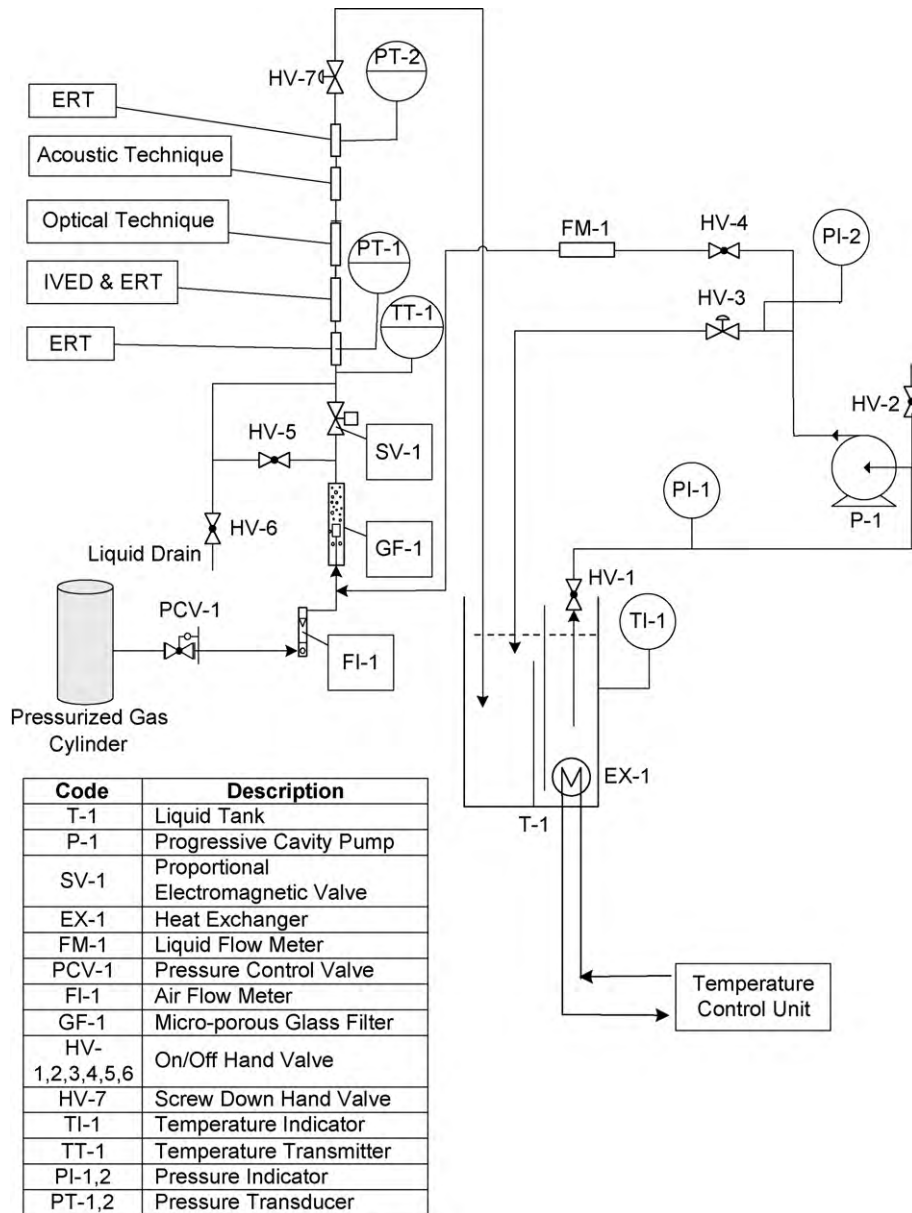


Fig. 1. Experimental set-up.

the combined effect of surfactant and electrolyte presence in the liquid phase on bubble size and/or bubble size distribution. Some early studies found that as inorganic salt concentration increases in a surfactant solution, coalescence time increases too [10,11]. In a recent work, Xu et al. [12] studied the effect of surfactant and electrolyte concentration on the size distribution and stability of microbubbles. They found that both have a negative effect on the bubble size, i.e., as any concentration increases bubbles of smaller size are observed.

The scope of the present study is to experimentally study bubbly flows, akin to those encountered during DCS in the human blood circulation. The latter corresponds to low gas volume fractions (below  $\sim 0.07$ ), sub-millimetre bubble sizes and low liquid velocities (below  $\sim 0.3$  m/s). Furthermore, the salinity and viscosity of the liquid phase must be within certain limits. An optical technique is employed to determine bubble sizes. This work is an exploratory, but necessary, effort to understand bubbly flows for the validation and tuning of the under-development electrical technique (In-Vivo Embolic Detector) for the characterization

of bubbly flows [4]. According to the above, surfactant is added to the liquid phase in order to reduce bubble size, while electrical conductivity is adjusted by adding small amounts of electrolyte(s). Consequently, new experimental data are acquired regarding the combined effect of the simultaneous presence of surfactant and electrolyte in the liquid phase and of the gas/liquid flow rates on bubble size distribution. The experiments are conducted in a test flow loop dimensionally representative of the vena cava of the human body.

## 2. Materials and methods

Measurements are conducted in a vertical co-current upward bubbly flow in a fully controllable flow loop made of Plexiglas® tubing, capable of generating steady and pulsatile flow conditions of various liquid/gas flow rates, gas fractions and bubble sizes. The loop is equipped with test sections accommodating electrical, optical, acoustical and pressure diagnostics (Fig. 1). There are two different electrical diagnostics. One is a modified 3D electri-

**Table 1**  
Physical properties of the employed liquids at 25 °C.

Liquid phase	Index	Surface tension (mN/m)		Viscosity (mPa s)	Electrical conductivity (mS/cm)
		25 ppm SDS	50 ppm SDS		
NaCl aqueous solution (5 mM)	W	65.0	64.0	1.0	0.5
PBS (NaCl 50 mM + Na <sub>3</sub> PO <sub>4</sub> 3 mM) aqueous solution (3%, v/v)	PBS	65.0	64.0	1.0	5.4
Glycerol (50%, w/w)/PBS (3%, v/v) aqueous solution	G/PBS	–	62.0	4.5	5.4

cal tomography technique (ERT) for checking the homogeneity of bubble flow across and along the tubing. The other is the under-development In-Vivo Embolic Detector (IVED) which is a very sensitive (down to  $\mu$ Vs) electrical probe capable of detecting electrical variations in reflection to bubble clouds variations [4]. It must be stressed that the present study focuses only on analysis of optical images. The liquid phase is recirculated through the flow loop by means of a progressive cavity pump (MD 025–6L, Motovario S.p.A.). The gas phase is injected through a cylindrical glass micro-filter-candle (ROBU<sup>®</sup>) with nominal pore size of 1.6  $\mu$ m located at the center of the bottom of the tube, where the two phases come in contact. It must be noted that the inside diameter of the tube is 21 mm identical to that of vena cava in the human body.

Experiments are performed at 37 °C, same as body temperature, in three different test liquids: (a) aqueous sodium chloride solution, hereafter called Water in the paper, resembling the electrical conductivity of tap water, (b) aqueous Phosphate buffered saline (PBS, Fluka Biochemika) solution, a liquid having the electrical conductivity of human blood, and (c) mixture of glycerol (purity >99.5%, Panreac) and PBS solution, a liquid having the electrical conductivity and viscosity of human blood (Table 1). Helium (purity >99.99%) is used as the gas phase in order to suppress gas dissolution to the flowing liquids and also reduce the gas/liquid surface tension. It should be noted that distilled water is used to prepare all liq-

uid phases. As already discussed, the addition of small amounts of a surface active agent into the liquid phase can influence the size of the produced bubbles. Thus, sodium dodecyl sulphate (SDS, purity >99.0%, Fluka Biochemika) at two different concentrations is added to the liquid phase in order to study its effect on the size of the bubbles inside the flow loop. It must be stressed that although the employed SDS concentrations yield comparable surface tension values which, in addition, are close enough to the helium/water surface tension value, they are still expected to affect differently the coalescence phenomena between bubbles.

The liquid flow rate ( $Q_L$ ) takes the value 600, 2100 or 6200 ml/min (steady flow), corresponding to liquid superficial velocities 3, 10 and 30 cm/s, as these values are representative of human blood circulation. On the other hand, the gas flow rate ( $Q_G$ ) is regulated between 1 and 240 ml/min so as the gas volume fraction inside the flow tube lies between  $\sim$ 0.001 and  $\sim$ 0.1. The gas volume fraction ( $\varepsilon$ ) is estimated by means of two differential pressure transducers (DP 15–20 and DP 15–30, Validyne<sup>®</sup>), placed before and after the location of electrical measurements.

A still digital camera (CANON EOS 350D) with an 8 MP resolution, equipped with a proper macro lens and three extension rings (13, 21 and 31 mm) in order to attain appropriate magnification, is employed. The camera is attached on a 3D translation table equipped with micro-metering mechanisms, because focusing to a

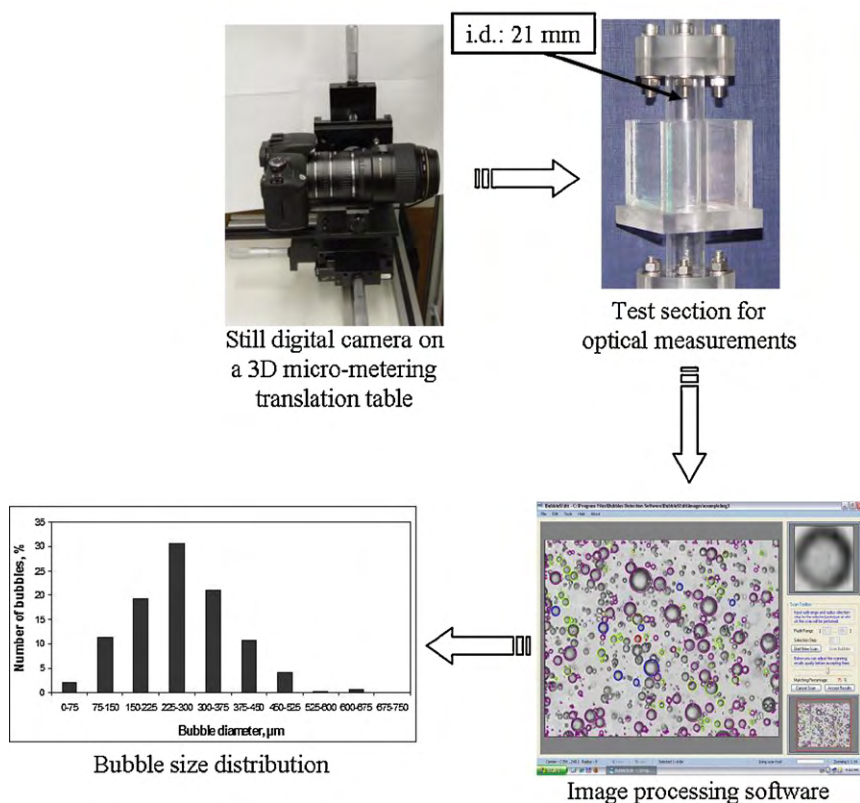


**Fig. 2.** Optical technique employed.

precise depth in the flow tube requires accurate lens displacement. In addition, the camera is placed on an anti-vibration table in order to avoid vibrations due to the liquid pump function. In order to discard optical distortion caused by the curved walls of the Plexiglas tube, a rectangular glass box filled with water has been mounted to the outer walls of the tube (Fig. 2) at a height of 75 cm above the gas sparger, while a wire 56  $\mu\text{m}$  thick is mounted at the outer surface of the tube as a reference scale. The camera uses the CMOS technology and is capable of saving images in raw format which enhances largely the spatial and intensity resolution of pixels. The high definition images acquired are then imported into a custom-made software [13] which is capable of estimating automatically the bubble size distribution. It should be accentuated that, in order to be statistically correct, more than 500 bubbles are measured at each experimental run [1].

### 3. Results and discussion

One of the first goals of the present work was to investigate whether the bubble size distribution is altered while moving from the wall region to the center of the tube. In the case of a vertical co-current upwards flow (as in the present study) it has been observed that smaller bubbles tend to move towards the wall, while large bubbles are preferably found in the centre due to the effect of the lift force, which depends at a great extent on bubble size (e.g. [14]). For this purpose, bubble size distributions were measured at three different radial locations of the tube, namely at the center of the tube, at distance  $R/2$  from the center, where  $R$  is the tube radius, and near the wall. Size distributions corresponding to these three locations are illustrated in Fig. 3 for one of the highest examined gas fractions, which can roughly be estimated by [15]:  $\varepsilon \approx Q_G/(Q_G + Q_L) = 0.097$ , where radial discrepancies are expected to be more profound. This is so because with such dense bubble population, bubble coalescence is more pronounced and, thus, bubbles of various sizes can co-exist in the flow. In the Figures that follow all size distributions are well fitted by log-normal curves as rather expected for this type of application (e.g. [7,16]). For comparison among data sets, the mean bubble diameter ( $d_{\text{mean}}$ ) of the displayed distributions is also included in the figures.

From Fig. 3, it is apparent that the bubble size distribution, and the size as well, remains practically unchanged at the various radial

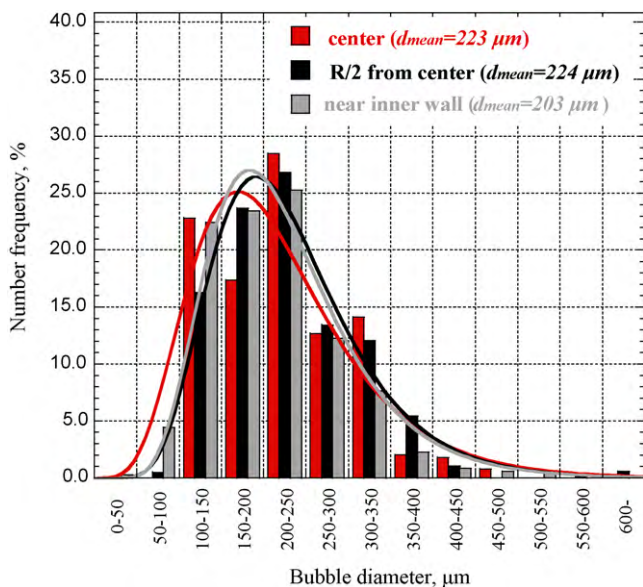


Fig. 3. Bubble size distribution for Water at three different radial positions of the tube ( $Q_L = 600$  ml/min,  $Q_G = 64.5$  ml/min, SDS concentration 50 ppm).

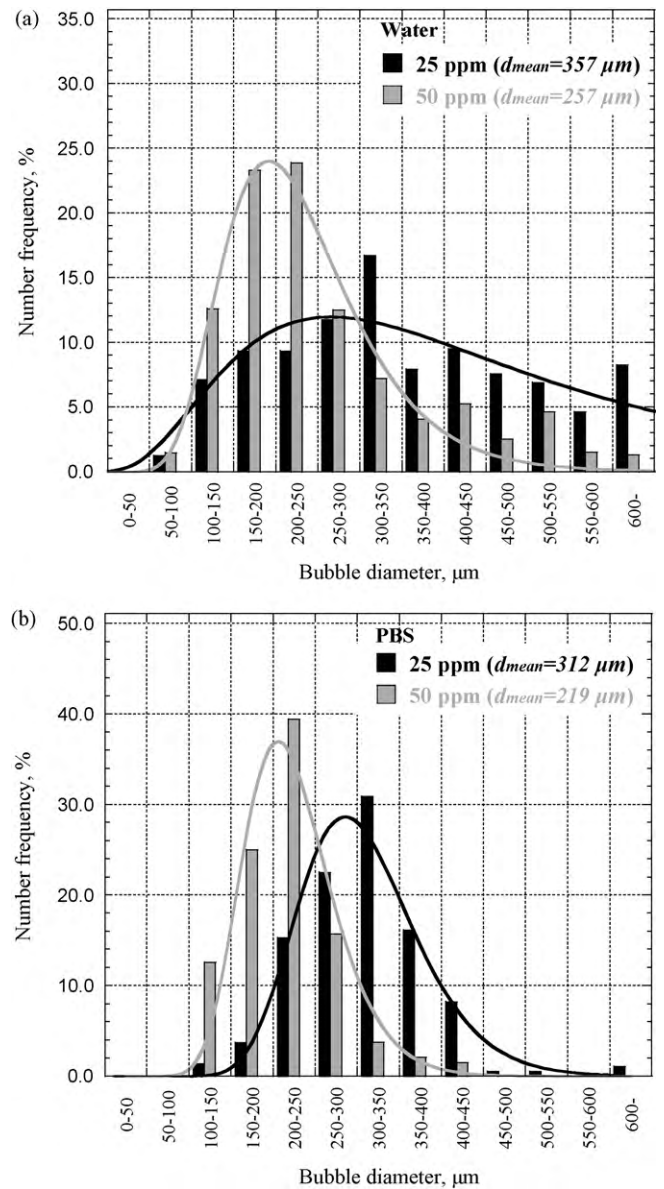


Fig. 4. Effect of surfactant concentration on bubble size distribution for (a) Water ( $Q_L = 600$  ml/min,  $Q_G = 11.3$  ml/min) and (b) PBS ( $Q_L = 6200$  ml/min,  $Q_G = 240.0$  ml/min).

positions. This indicates that, at this height of the tube, a radial homogeneity exists, meaning that bubbles of all sizes are evenly spread across the tube cross section. Consequently, it was decided the size distributions to be determined near the inner wall of the tube for all experimental runs of this work.

Fig. 4 illustrates the effect of the surfactant concentration on bubble size distributions for (a) Water ( $\varepsilon \approx 0.018$ ) and (b) PBS ( $\varepsilon \approx 0.038$ ). One can readily see that as the surfactant concentration increases from 25 to 50 ppm in both liquids, the size of the bubbles decreases appreciably, while at the same time the size distribution becomes narrower, indicating the strong influence of surfactant addition on bubble size. At such low surfactant concentrations, the surface tension of the solution is not so different from the pure water value. Yet, for pure water bubbles were above 1.5 mm in diameter with most of them clearly distorted from sphericity (results not shown). This manifests that the observed smaller bubbles with increasing surfactant concentration is due to coalescence inhibition rather than to surface tension effects.

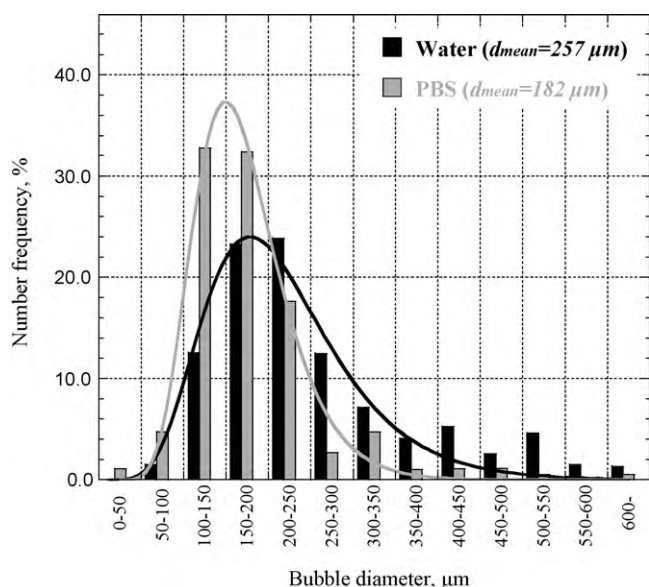


Fig. 5. Effect of liquid salinity on bubble size distribution ( $Q_L = 600$  ml/min,  $Q_G = 11.3$  ml/min, SDS concentration 50 ppm).

Another observation from Fig. 4 is that in Water the bubble size distributions are broader than in PBS. Accordingly, the mean bubble size for Water is higher than for PBS. The above most likely imply interaction of the surfactant molecules with the electrolyte(s) in PBS enhancing coalescence inhibition.

To better show the effect of liquid salinity on bubble size distribution, Fig. 5 compares a representative pair of size distributions in Water and PBS obtained under exactly the same operating conditions (gas and liquid flow rate,  $\varepsilon \approx 0.018$ ) and SDS concentration. It is evident that when PBS, which has much higher salinity, is employed bubbles of much smaller sizes are observed in the tube. Similarly, Marrucci and Nicodemo [17] and Keitel and Onken [18], who measured the size distributions in a bubble column by employing various aqueous salt solutions as the liquid phase, found that as the salt concentration increases bubble size decreases at a great extent and attributed this behaviour to electrical repulsive forces which hinder coalescence between bubbles brought in contact by the liquid motion. It seems that, despite the surfactant (SDS) existence in the liquid phase, addition of an electrolyte can further promote the coalescence hindrance and, thus, reduce bubble size, a behaviour observed by others investigators as well (e.g. [10–12]).

Fig. 6 shows the effect of gas flow rate on the resultant size distributions for two of the employed test liquids. For the same liquid flow rate, as the gas flow rate increases the size distribution is somewhat shifted to higher sizes, i.e., the number frequency of bubbles with larger sizes increases. The increase of gas flow rate yields more bubbles from the sparger and, thus, augments their population in the tube. Consequently, the frequency of collisions between bubbles increases and bubble coalescence becomes more pronounced leading to relatively larger bubble sizes inside the tube, a behaviour also observed by other investigators (e.g. [17]).

As already mentioned, in this work there have been no tests with varying liquid flow rate at constant gas flow rate since the aim was to adjust the gas volume fraction inside the tube to roughly constant values. Consequently, the effect of the liquid flow rate on the bubble size cannot be clarified. However, one should expect that the liquid flow rate plays a dual role. As it is increased, the tearing effect during bubble formation becomes more pronounced. Bubbles are forced to detach from the sparger at an earlier stage of their expansion due to the increased liquid velocity and, thus, bubbles of smaller size are produced [19]. On the other hand, as the liquid flow

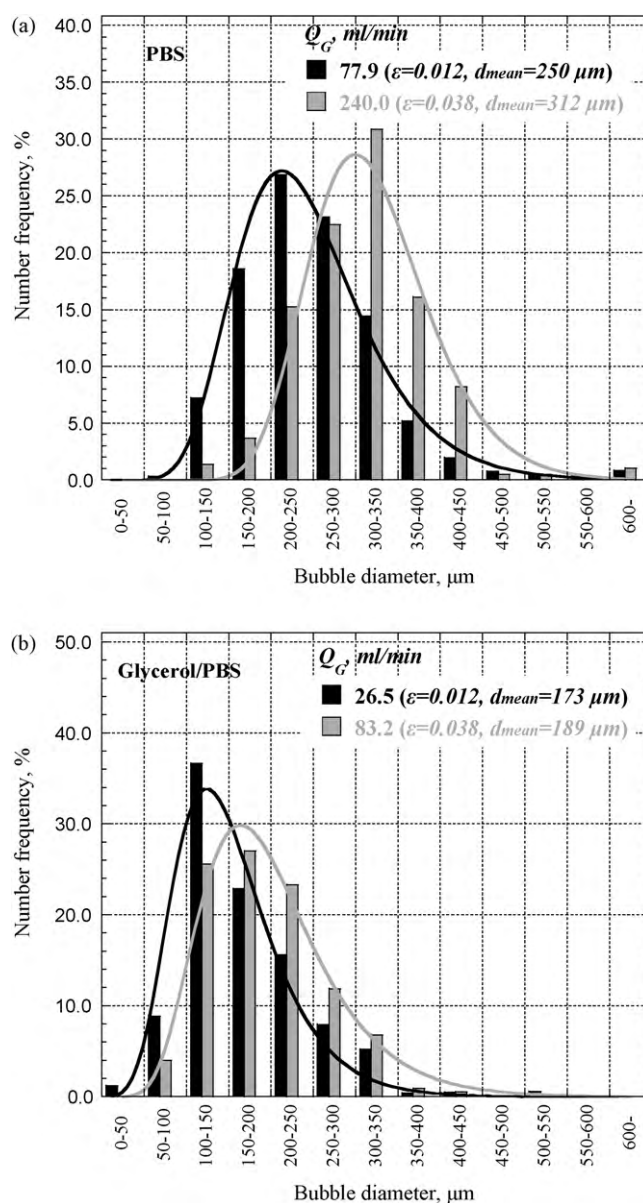


Fig. 6. Effect of gas flow rate on bubble size distribution for (a) PBS ( $Q_L = 6200$  ml/min, SDS concentration 25 ppm) and (b) glycerol/PBS ( $Q_L = 2100$  ml/min, SDS concentration 50 ppm).

rate is increased, turbulence in the liquid also increases, enhancing collisions and, consequently, coalescence between bubbles, which, in turn, favours the formation of larger bubbles.

In Fig. 7 the effect of viscosity of the liquid phase on the bubble size distribution is depicted. The two liquid phases, namely PBS and G/PBS solution, have similar surfactant and salt concentration, while their surface tension values are practically the same. However, the G/PBS solution is about 5 times more viscous than the PBS. In Fig. 7, one can see that the size distribution is marginally affected by the liquid viscosity in the examined range. Ruzicka et al. [20], who studied the effect of liquid viscosity on a bubble column performance, assert that viscosity plays a dual role. At low viscosities, as in the present case, as viscosity increases, the larger drag forces are not strong enough to promote coalescence and, as a result, have no effect on the size distribution. On the other hand, at a higher viscosity, the tendency to coalescence and polydispersity prevails over the drag reduction and the uniformity is broken by big bubbles.

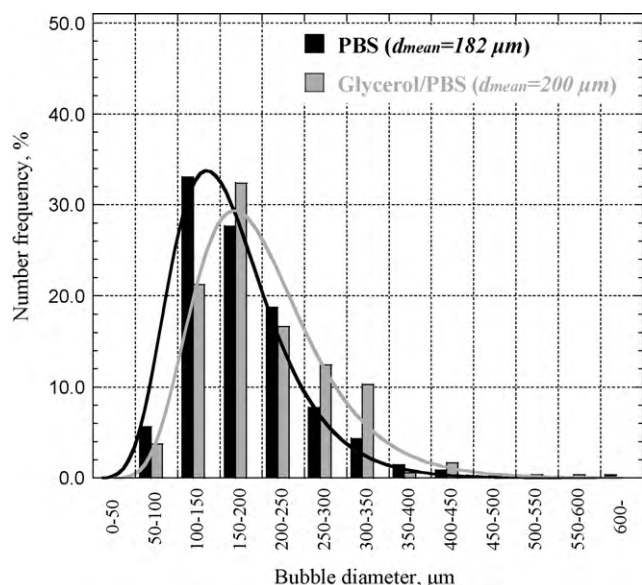


Fig. 7. Effect of liquid viscosity on bubble size distribution ( $Q_L = 600$  ml/min,  $Q_G = 51.2$  ml/min, SDS concentration 50 ppm).

#### 4. Conclusions

In the present work, experiments in a bubbly flow comparable to that observed during DCS in the human body were conducted. The influence of the simultaneous presence of surfactant (SDS) and electrolyte in the liquid phase on the bubble size distribution was studied. The size distribution seems to be practically independent of the radial position of the tube and the viscosity of the liquid phase, while it shows strong dependency on both surfactant and electrolyte concentration. When surfactant and electrolyte co-exist, bubble coalescence is hindered to a greater extent than if they were alone in the liquid phase. Finally, bubble size distribution appears to be slightly contingent on the flow rates of the two phases.

Further experiments are needed, and are indeed currently in progress, employing higher surfactant concentrations and pulsatile flow conditions in order to, on the one hand, obtain even smaller bubbles and, on the other hand, correctly simulate the blood flow conditions in the human blood circulation system.

#### Acknowledgements

Financial support by the European Space Agency through the project "In-Vivo Embolic Detector, Phase IIIa" (ESA GSTP CCN/6-18354/05/NL/PA) and "Convective Boiling and Condensation" (ESA-AO-2004-PCP-111/ELIPS-2) is gratefully acknowledged.

This work is conducted under the umbrella of the COST P21 action: Physics of Droplets. This paper is part of the O3E $\Delta$ 376 research project, implemented within the framework of the "Reinforcement Programme of Human Research Manpower" (PENED) and co-financed by National and Community Funds (25% from the Greek Ministry of Development-General Secretariat of Research and Technology and 75% from E.U.-European Social Fund).

#### References

- [1] W.D. Deckwer, Bubble Column Reactors, John Wiley and Sons, England, 1992.
- [2] R.D. Vann, E.D. Thalmann, Decompression physiology and practice, in: P. Bennett, D. Elliot (Eds.), The Physiology and Medicine of Diving, W.B. Saunders Company, London, 1993.
- [3] V.P. Katuntsev, Yu.Yu. Osipov, A.S. Barer, N.K. Gnoevaya, G.G. Tarasenkov, The main results of EVA medical support on the Mir Space Station, Acta Astronaut. 54 (2004) 577–583.
- [4] T.D. Karapantsios, M. Kostoglou, S.P. Evgenidis, From single bubbles on solid surfaces to massive bubbly flows during decompression sickness, J. Gravit. Physiol., in press.
- [5] B.A. Hills, D.C. Grulke, Evaluation of ultrasonic bubble detectors in vitro using microbubbles at selected velocities, Ultrasonics 13 (1975) 181–184.
- [6] T.J. Hanratty, T. Theofanous, J.-M. Delhaye, J. Eaton, J. McLaughlin, A. Prosperetti, S. Sundaresan, G. Tryggvason, Workshop findings, Int. J. Multiphase Flow 29 (2003) 1047–1059.
- [7] E. Camarasa, C. Vial, S. Poncin, G. Wild, N. Midoux, J. Bouillard, Influence of coalescence behaviour of the liquid and of gas sparging on hydrodynamics and bubble characteristics in a bubble column, Chem. Eng. Process. 38 (1999) 329–344.
- [8] S.S. Alves, C.I. Maia, J.M.T. Vasconcelos, A.J. Serralheiro, Bubble size in aerated stirred tanks, Chem. Eng. J. 89 (2002) 109–117.
- [9] R. Lessard, S. Zieminski, Bubble coalescence and gas transfer in aqueous electrolytic solutions, Ind. Eng. Chem. Fundam. 10 (1971) 260–269.
- [10] D. Li, J.C. Slattery, Experimental support for analysis of coalescence, AIChE J. 34 (1988) 862–864.
- [11] M.K. Kumar, P. Ghosh, Coalescence of air bubbles in aqueous solutions of ionic surfactants in presence of inorganic salt, Chem. Eng. Res. Des. 84 (2006) 703–710.
- [12] Q. Xu, M. Nakajima, S. Ichikawa, N. Nakamura, P. Roy, H. Okadome, T. Shiina, Effects of surfactant and electrolyte concentrations on bubble formation and stabilization, J. Colloids Interf. Sci. 332 (2009) 208–214.
- [13] X. Zabulis, M. Papara, A. Chatziargyriou, T.D. Karapantsios, Detection of densely dispersed spherical bubbles in digital images based on a template matching technique: application to wet foams, Colloids Surf. A: Physicochem. Eng. Aspects 309 (2007) 96–106.
- [14] D. Lucasa, E. Kreppera, H.-M. Prasserb, Use of models for lift, wall and turbulent dispersion forces acting on bubbles for poly-disperse flows, Chem. Eng. Sci. 62 (2007) 4146–4157.
- [15] J.R. Thome, Engineering Data Book III, Wolverine Tube Inc., 2004, Available at: <http://www.wlv.com/products/databook/db3/DataBookIII.pdf>.
- [16] N.A. Kazakis, A.A. Mouza, S.V. Paras, Experimental study of bubble formation at metal porous spargers: effect of liquid properties and sparger characteristics on the initial bubble size distribution, Chem. Eng. J. 137 (2008) 265–281.
- [17] G. Marrucci, L. Nicodemo, Coalescence of gas bubbles in aqueous solutions of inorganic electrolytes, Chem. Eng. Sci. 22 (1967) 1257–1265.
- [18] G. Keitel, U. Onken, Inhibition of bubble coalescence by solutes in air/water dispersions, Chem. Eng. Sci. 37 (1982) 1635–1638.
- [19] K. Loubiere, V. Castaignede, G. Hebrard, M. Roustan, Bubble formation at a flexible orifice with liquid cross-flow, Chem. Eng. Process. 43 (2004) 717–725.
- [20] M.C. Ruzicka, J. Drahos, P.C. Mena, J.A. Teixeira, Effect of viscosity on homogeneous–heterogeneous regime transition in bubble columns, Chem. Eng. J. 96 (2003) 15–22.